RSC Advances




ROYAL SOCIETY OF CHEMISTRY

www.rsc.org/advances

# $RuO_2$/MWCNT/ Stainless Steel Mesh as a novel positive electrode in vanadium redox flow batteries

Fereydoon Gobal, Masoud Faraji *

Department of Chemistry, Sharif University of Technology, P.O. Box 11365-9516, Tehran, Iran

**Abstract**

The present work describes the preparation and electrochemical characterization of RuO2/MWCNT/Stainless Steel Mesh (SSM) electrode as compared with a MWCNT/SSM electrode in the positive half-cell of a Vanadium Redox Flow Battery (VRFB). The electrochemical characterization of prepared electrode was carried out using cyclic voltammetry (CV), electrochemical impedance spectroscopy (EIS) and galvanostatic charge/discharge procedures. The electrochemical activity of MWCNT/SSM modified with RuO2 as positive electrode in a VRFB was notably improved. The RuO2-included electrodes demonstrated high peak current ratio, small peak potential difference and high electron transfer rate constant, confirming excellent electro-catalytic activity and reversibility. These good electrochemical results, together with the long term stability of the prepared electrode, represent a significant step forward in the development of highly effective positive electrode materials for VRFBs.

**Keywords:** *Vanadium redox flow batteries, MWCNT, $RuO_2$, Stainless Steel Mesh*

## 1. Introduction

Among a wide range of energy storage technologies, redox flow batteries (RFB) offer several unique advantages, including the system scalability, long cycle life, and high energy efficiency [1]. RFBs are electrochemical energy storage devices where the energy is stored and converted through chemical changes of species dissolved in a working fluid. Among various kinds of RFB, vanadium RFB (VRFB) consisting of $[VO]^{2+}/[VO_2]^{+}$ redox couples in the positive electrode and $[V]^{3+}/[V]^{+2}$

redox couples in the negative electrode has been mostly considered due to its independently tunable power and capacity, long cycle life, low operation cost, and high energy efficiency [2-4]. It is known that the positive electrode reactions are slower and more complicated than that of $[V]^{3+}/[V]^{2+}$redox couples (negative electrode), meaning that the former is the determining reaction [3]. So, much attention has been paid to the fabrication of new positive electrode materials for VRFBs. Recently, MWCNTs has been introduced as a new positive electrode material for VRFBs because of its large reactive surface area, high stability in acidic solutions and relatively low cost [5-8]. However, in spite of such advantages, practical use of the MWCNT-based electrodes as positive electrode for VRFB has been restricted because of its low electrochemical performance [6]. Despite low energy efficiency, it seems that MWCNT-based electrodes still possess high potential for further investigation as positive electrode especially if modification of the surface of pristine MWCNT could be performed. Recently, Friedl et al. investigated electron transfer kinetics of the $[VO]^{2+}/[VO_2]^{+}$ reaction on functionalized MWCNTs [5]. They concluded that defunctionalized MWCNT promotes the $[VO]^{2+}/[VO_2]^{+}$ redox reaction better than MWCNT having surface oxygen groups. The observed order of reaction rates contradicts earlier reports [6, 7] and indicates that the $[VO]^{2+}/[VO_2]^{+}$ reaction is not catalyzed in the presence of the surface functional groups. However, in a recent study, Li et al. reported that the MWCNTs treated in the air at 600 °C shows better electrochemical performances for the $[VO]^{2+}/[VO_2]^{+}$ redox reaction than untreated MWCNTs[8]. Despite these contradictions in mentioned literatures, it seems that reliable treatments on the surface of pristine MWCNTs must be developed to improve the electrochemical activity of MWCNT–based electrodes as the positive electrode of the VRFBs. Some investigations showed that the electrochemical activity of $[VO]^{2+}/[VO_2]^{+}$ redox couples can be facilitated by the loading of $WO_3$ on carbon paper [9], $PbO_2$ on graphite felt [10] and $Mn_3O_4$ on carbon felt [11]. According to their

results, $WO_3$, $PbO_2$ and $Mn_3O_4$ play critical roles in activating redox reactions of vanadyl ions. However, these electrocatalysts may suffer of low stability in acidic solutions for long time applications and also low electrochemical performance. Compared to these electrocatalysts, $RuO_2$ not only has high stability in acidic solutions, but also has high electrocatalytic activity that may be suitable for VRFB applications [12,13]. The possibility of ruthenium oxides ($RuO_x$ or $RuO_xH_y$) acting as electro-catalyst has recently attracted both interests and debates [13]. One reason for the apparent inconsistencies in the reported literature may be due to the various forms of ruthenium oxide with different oxidation and hydrous states having different electrochemical characteristics. Oxides with tetravalent ruthenium (e.g. $RuO_2$, $RuO_2$. $nH_2O$, $H_{0.2}RuO_{2.1}$ .n $xH_2O$) are known to be electrochemically stable within the hydrogen and oxygen evolution limits, thereby are promising electrode materials for electrochemical supercapacitors, fuel cell and also for analytical applications [14-16].

The present work is mainly focused on the preparation and electrochemical investigation of $RuO_2$/MWCNT/Stainless Steel Mesh as positive electrode material for vanadium redox flow systems. To the best our knowledge, no reports considering incorporation of an electrocatalyst onto the surface of MWCNT as positive electrode material for VRFB has been published. Stainless Steel Mesh (SSM) was used as supporting material for deposition of MWCNT because of specific two-dimensional structure (low thickness and high lateral dimension) that could increase the vanadium ions permeation in the electrode. Additional advantages of SSM as supporting electrode are its unique thermal, mechanical and electrical properties and low cost compared to other supporting electrode materials like glassy carbon or graphite, which used to be employed in VRFBs. It has been known that using of metal meshes as supporting electrode at various applications has a positive influence in improving the electron transfer by providing a better conductivity throughout the

electrode surface [17, 18]. It should be noted that different types of metal meshes have been widely used as supporting material at catalysts [19], fuel cells [20, 21], batteries [22] and solar cells [23].

## 2. Experimental procedure

### 2.1. Preparation of the $RuO_2$/MWCNT/SSM electrode

SSM (AISI304) of mesh 100 with wire diameter of 0.2 mm was cut into 1cm×3cm ribbons and was used as support material for developing working electrodes. 0.2 g of conventional MWCNTs and 0.02 g of polyvinyl chloride (PVC) as binder was dispersed in 3 ml THF by sonication for 40 min. The suspended solution was painted on SSM ribbons followed by drying at 60 °C. The black colored, homogeneous and adherent MWCNTs coatings were successfully obtained on the SSM substrate and denoted as MWCNT/SSM electrode. Various methods such as solution chemistry techniques, electrochemical deposition, sputtering techniques, and organometallic chemical vapor deposition have been employed to prepare ruthenium oxide films [24]. The electrodeposition methods offer a number of advantages compared with other techniques. For instance, the preparation procedure is relatively simple, and the growth of film can be easily modulated by varying the experimental parameters such as applied potential, electrolyte compositions and deposition time [24,25]. Among various methods for electrodeposition of $RuO_2$ films, cathodic deposition is a better choice since deposition rate and current efficiency are high and uniform coatings of the $RuO_2$ film can be obtained [24,25]. Cathodic electrodeposition of $RuO_2$ onto the MWCNT/SSM electrode was carried out galvanostatically according to [24- 26] in a plating bath containing 20 mM $RuCl_3$, 0.1 M KCl and 0.01 M HCl at a constant current of 20 mA for the duration of 100 s in a two-electrode system using MWCNT/SSM electrode as a working electrode and Pt as a counter electrode at room temperature. The pH value of the plating bath was kept at 2.0 by adding HCl or KOH aqueous solution throughout the electrodeposition. XPS result mentioned in the literatures[24,25] indicate that the species on the

cathodically deposited film contained ruthenium hydroxides/oxides and some amount of Ru(0), so cyclic voltammetry (two scans) was used for oxidation of metallic Ru at surface to $RuO_2$ in 2.0 M $H_2SO_4$ solution in voltage range of -0.5 to 1.5 V versus Ag/AgCl. Finally, the electrodes were rinsed thoroughly several times with water and dried in an oven at 60 °C for 1 h in air. The weight of the electrodes was measured by a microbalance. The mass of MWCNT+ $RuO_2$ deposited on the electrodes was about 0.04 g where error of around 5% is conceivable. Also, electrodeposition of $RuO_2$ on the bare SSM substrate was carried out at the same conditions to investigate the influence of MWCNT on electrochemical activity of the electrodes.

It has been reported that corrosion rate of stainless steel immersed in 1 M $H_2SO_4$ is below 0.1 mm/year at ambient temperature [27, 28]. Moreover, it has been widely known that the sandwiched structure of polymer composites/CNT deposited on 304 SS endows the steel further good corrosion resistance in high concentrations of $H_2SO_4$ solutions [29-31]. Therefore, it can be expected that $RuO_2$/MWCNT sandwiched structure deposited on SSM can be an appropriate coating for corrosion protection of SSM in $H_2SO_4$ solutions, enabling it to be employed in VRFBs studies.

### 2.2. Characterization and electrochemical studies

Morphological studies were carried out by a scanning electron microscope (Philips, Model XL30). Chemical compositions were determined by EDX in a scanning electron microscope (VEGA\\Tescan). Cyclic voltammetry, galvanostatic charge/discharge and electrochemical impedance studies were carried out using Voltalab10 electrochemical system. All electrochemical studies were performed in a conventional three electrode cell using platinum foil as a counter electrode where all potentials are reported against Ag/AgCl reference electrode at room temperature.

## 3. Results and discussion

### 3.1. Morphology characterization

The SEM images in Fig. 1 show significant differences in the morphologies of the coatings. Fig. 1a shows the SEM image of MWCNT/SSM electrode where MWCNTs have an even distribution on the surface of SSM. Fig. 1b shows the MWCNT/SSM electrode with high magnification. As it can be seen in Fig. 1b, MWCNT film has covered the entire surface of SSM and pieces of randomly entangled MWCNTs form a homogeneous film. Fig. 1c shows MWCNT/SSM structure coated with $RuO_2$ where $RuO_2$ nanoparticles (in range of 50 to 100 nm) have been deposited on the MWCNT/SSM and high surface area of $RuO_2$ is thus available. As seen from Figs. 1b and 1c, $RuO_2$/MWCNT deposits entirely cover the surface of SSM substrate, so the underlying surface is entirely deprived of the electrolyte and the corrosion of SSM is thus highly unlikely. Fig. 1d shows the EDX spectrum of the $RuO_2$/MWCNT/SSM electrode that confirms the presence of the Ru on MWCNT/SSM. As seen from Fig. 1d, carbon is the major element which is derived from MWCNT and small amounts of Ru element that can be identified in EDX spectrum. Fig. 1e shows a typical XRD pattern of cathodically deposited $RuO_2$ thin film on MWCNT/SSM. The X-ray pattern of the MWCNT displays the presence of two peaks at $25.80^{\circ}$ and $42.75^{\circ}$ assigned to (002) and (100) diffractions corresponding to the interlayer spacing of the nanotube and reflection of the carbon atoms, respectively, in good agreement with that of the previous literature [32]. There is a weak peak from metallic Ru at $38^{\circ}$ [33] and no identification of any crystalline phase of $RuO_2$ in the film. So the XRD result clearly indicates that the film grown on the MWCNT/SSM electrode has amorphous characteristics i.e. formation of unstructured ruthenium oxide film. Similar results are also observed for other literatures, where $RuO_2$ was deposited on various substrates [34, 35]. Also, It has been reported that when the annealing temperature is raised to 400 °C, three sharp peaks located at $28^{\circ}$, $36^{\circ}$, and $54^{\circ}$ corresponding to anhydrous $RuO_2$ (1 1 0), (1 0 1) and (2 1 1) orientations are clearly observed, indicating long-range crystalline order[36].

3.2. CV and EIS analysis

Fig. 2a shows the cyclic voltammograms of $RuO_2$/MWCNT/SSM electrode and MWCNT/SSM electrode at scan rate of 20 mV $s^{-1}$ in 0.14 M $[VO_2]^+$ + 2 M $H_2SO_4$ solutions. There are significant differences in the peak potentials ($E_{pa}$ and $E_{pc}$) and peak currents ($I_{pa}$ and $I_{pc}$) values, which reflect substantial differences in the electrochemical performance. The peak currents due to the redox processes of $[VO]^{2+}/[VO_2]^+$ on the MWCNT/SSM modified with $RuO_2$ are 88 and -85 mA, respectively, whereas the corresponding peak currents for MWCNT/SSM electrode are 58 and -46 mA, respectively. The oxidation and reduction peaks corresponding to a $[VO]^{2+}/[VO_2]^+$ couple for MWCNT/SSM electrode appear at approximately 1.3 and 0.55 V vs. Ag/AgCl, respectively, whereas, the oxidation and reduction potentials on the $RuO_2$/MWCNT/SSM electrode were 1.25 V and 0.6 V, respectively. Therefore, the $RuO_2$/MWCNT/SSM electrode exhibits the higher anodic and cathodic peak current and the lower $\Delta E_p$ values, reflecting some improvement in the electrochemical activity towards $[VO]^{2+}/[VO_2]^+$ redox reactions[37, 38]. Furthermore, the ratio of oxidation peak current and reduction peak current ($I_{pa}/I_{pc}$) of $RuO_2$/MWCNT/SSM is close to 1, indicating that the electrode containing $RuO_2$ exhibits better electrochemical reversibility for $[VO]^{2+}/[VO_2]^+$ redox reaction[38, 39]. As can be seen from Fig. 2a, the SSM substrate loaded with $RuO_2$ does not exhibit suitable electrochemical activity toward the $[VO]^{2+}/[VO_2]^+$ redox reaction, which may be due to the poor conductivity of $RuO_2$ loaded on SSM substrate. Moreover, due to small loading of $RuO_2$ on SSM and contact possibility between electrolyte and SSM, corrosion problems of the SSM may be predictable. Based on mechanisms proposed for some electro-catalysts which used to be employed in VRFBs [9-11], the functional group $-Ru^{\partial+}=O$ on the surface of $RuO_2$ molecule may be the key factor for the remarkable improvement of electrochemical activities. The catalytic mechanism is presumed as shown in Fig. 2b. In short, MWCNT provides large electrode surface area, good

conductivity and parts of the active sites. $RuO_2$ provides more active center to improve the adsorption of activated species and decrease the polarization of electrode reactions, so the $RuO_2$/MWCNT exhibited excellent electrochemical activity toward the $[VO]^{2+}/[VO_2]^{+}$ redox reaction.

Fig. 3 displays the EIS plots of MWCNT/SSM electrode with and without $RuO_2$ in 0.14 M $[VO]^{2+}$ + 0.14 M $[VO_2]^{+}$ + 2 M $H_2SO_4$ solution at the open-circuit potential. The Nyquist plots include a semicircle terminating to a straight line and indicating the involvement of charge transfer and diffusion steps [40, 41]. It is clearly shown that the charge transfer resistance is greatly decreased after the loading of $RuO_2$ on the MWCNT/SSM, confirming the electrocatalytic effect provided by the $RuO_2$ nanoparticles in combination with the MWCNT/SSM electrode, which is in agreement with results obtained in cyclic voltammetry studies.

In order to investigate the $[VO]^{2+}/[VO_2]^{+}$ redox processes on the $RuO_2$/MWCNT/SSM electrode, CVs were recorded at different scan rates in 0.14 M $[VO_2]^{+}$ + 2 M $H_2SO_4$ electrolyte (Fig. 4a). With the scan rate increasing, the peak potential separation changes slightly, suggesting the redox reactions of $[VO]^{2+}/[VO_2]^{+}$ couple are quasi-reversible on this electrode[6, 9, 42, 43]. A linear relationship between the anodic and cathodic peak currents and the square root of the scan rate (Fig. 4b) observed on the $RuO_2$/MWCNT/SSM indicates that the oxidation of $[VO]^{2+}$ and the reduction of $[VO_2]^{+}$ are mainly controlled by their diffusion from the electrolyte to the electrode surface [44]. Fig. 5a shows cyclic voltammograms of the $RuO_2$/MWCNT/SSM electrode in 2 M $H_2SO_4$ solution in the presence of various concentrations of V(IV)/V(V) at a potential sweep rate of 20 mV $s^{-1}$. Increasing the concentration causes a proportional enhancement of peaks of both oxidation and reduction, which is shown in Fig. 5b.

3.3. Charge-discharge test

In order to investigate the effect of $RuO_2$ on the electrochemical performance, the charge-discharge curves of half-cell of $RuO_2$/MWCNT/SSM and MWCNT/SSM as positive electrode were compared in a conventional three electrode cell in 0.14 M V(IV) + 0.14 M V(V) + 2 M $H_2SO_4$ solution at the current density of 500 mA $g^{-1}$ (current/ mass of $RuO_2$+MWCNT). It can be seen from Fig. 6, the half-cell using the modified positive electrode has higher specific discharge capacity (49 mAh $g^{-1}$) than the MWCNT/SSM positive electrode (22 mAh $g^{-1}$). Furthermore, the curve of the half-cell with $RuO_2$-modified MWCNT/SSM as positive electrode has a low charge voltage plateau and high discharge voltage plateau, indicating a lower charge voltage and higher energy storage efficiency for the VFB [45,46]. All these factors confirm that modified electrode can be a promising alternative for improving the VRFB. The typical charge discharge curves of the half-cell with $RuO_2$-modified MWCNT/SSM at current densities were tested and are presented in Fig. 7. It is found that the half-cell maintains high charge–discharge performance under different rates. Fig. 8 shows charge/discharge curves of the first cycle and a similar cycle after 10 days of sample being used in various electrochemical studies at the current density of 500 mA $g^{-1}$. A partial decrease in capacitance from 49 mAh $g^{-1}$ to 45 mAh $g^{-1}$ has been observed showing 91% perseverance of specific discharge capacity. Data presented in Fig. 8 indicates that the electrode retains its activity over extended period of time and use in various experiments and numerous cycles of charge/discharge.

**4. Conclusion**

$RuO_2$/MWCNT/SSM electrode was presented as electrochemical active material for $[VO]^{2+}/[VO_2]^{+}$ redox couple for VRFBs. The composite electrode is suitable for use as positive electrode in VRB and exhibits better performances with a higher peak current density, lower $\Delta E_p$ value and a lower charge transfer resistance of the electrode reactions in comparison with MWCNT/SSM electrode.

The improvement of the electrochemical activity of the electrode can be ascribed to catalytic effect of $RuO_2$ nanoparticles dispersed on the surface of the MWCNTs. The specific capacitance maintained 91% of initial value upon 10 days of prolonged studies, suggesting a promising positive electrode material for VRFBs.

**Acknowledgment**

The authors wish to express thanks to the office of vice chancellor of research of Sharif University of Technology for the financial support.

**References**

[1] X.L. Zhou, T.S. Zhao, L. An, L. Wei and C. Zhang, Electrochim. Acta, 2015, 153, 492-498.

[2] S. Jeong, S. Kim and Y. Kwon, Electrochim. Acta, 2013, 114, 439-447.

[3] S.C. Raghu, M. Ulaganathan, T.M. Lim and M.S. Kazacos, J. Power Sources, 2013, 238, 103-108.

[4] J.G. Lee, S.J. Park, Y. Cho and Y.G. Shul, RSC Adv., 2013, 3, 21347-21351.

[5] J. Friedl, C.M. Bauer, A. Rinaldi and U. Stimming, Carbon, 2013, 63, 228-239.

[6] W. Li, J. Liu and C. Yan, Carbon, 2011, 49, 3463-3470.

[7] L. Yue, W. Li, F. Sun, L. Zhao and L. Xing, Carbon, 2010, 48, 3079-3090.

[8] W. Li, J. Liu and C. Yan J. Solid State Electrochem., 2013,17,1369-1376.

[9] C. Yao, H. Zhang, T. Liu, X. Li and Z. Liu, J. Power Sources, 2012, 218, 455-461.

[10] X. Wu, H. Xu, L. Lu, H. Zhao, J. Fu, Y. Shen, P. Xu and Y. Dong, J. Power Sources, 2014, 250, 274-278.

[11] K.J. Kim, M.S. Park, J.H. Kim, U. Hwang, N.J. Lee, G. Jeong and Y.J. Kim, Chem. Commun., 2 012, 48, 5455-5457.

[12] J.H. Ma, Y.Y. Feng, J. Yu, D. Zhao, A.J. Wang and B.Q. Xu, J. Catal., 2010, 275, 34-44.

[13] W. Sugimoto, T. Saida and Y. Takasu, Electrochem. Commun., 2006, 8, 411-415.

[14] Z. Chen, X. Qiu, B. Lu, S. Zhang, W. Zhu and L. Chen, Electrochem. Commun., 2005, 7, 593-596.

[15] V. Barranco, F. Pico, J. Ibanez, M.A. Lillo-Rodenas, A. Linares-Solano, M. Kimura, A. Oya, R.M. Rojas, J.M. Amarilla and J.M. Rojo, Electrochim. Acta., 2009, 54, 7452-7457.

[16] H.R. Zare, S.H. Hashemi and A. Benvidi, Anal. Chim. Acta, 2010, 668, 82-187.

[17] L. Lipp and D. Pletcher, Electrochim. Acta, 1997, 42, 1101-1111.

[18] M. Sharma, P. Jain, J. L. Varanasi, B. Lal, J. Rodríguez, J. M. Lema and P. M. Sarma, Bioresour. Technol., 2013, 150,172-180.

[19] T.T. Vu, L. Río, T. Valdés-Solís and G. Marbán, J. Hazard. Mater., 2013, 247, 126-134.

[20] S. Basu, A. Agarwal and H. Pramanik, Electrochem. Commun., 2008, 10, 1254-1257.

[21] Y. Zhang, J. Sun, Y. Hu, S. Li and Q. Xu, J. Power Sources, 2013, 239, 169-174.

[22] W.H. Zhu, P. J. Durben and B. J. Tatarchuk, J. Power Sources, 2002, 111, 221-231.

[23] X. Huang, P. Shen, B. Zhao, X. Feng, S. Jiang, H. Chen, H. Li and S. Tan, Sol. Energy Mater. Sol. Cells, 2010, 94, 1005-1010.

[24] J.J. Jow, H.J. Lee, H.R. Chen, M.S. Wu and T.Y. Wei, Electrochim. Acta, 2007, 52, 2625-2633.

[25] J.M. Sieben, E. Morallón and D. Cazorla-Amorós, Energy, 2013, 58, 519-526.

[26] I. Zhitomirsky and L. Gal-Orm, Mater. Lett., 1997, 31, 155-159.

[27] I. Iliyasu, D.S. Yawas and S.Y. Aku, Adv. Appl. Sci. Res., 2012, 3, 3909-3915.

[28] B. Jegdic, D. M. Drazic and J. P. Popic, J. Serb. Chem. Soc., 2006, 71, 543-551.

[29] Y.B. Lee, C.H. Lee and D.S. Lim, Int. J. Hydrogen Energ., 2009, 34, 9781-9787.

[30] A.E.A. Hermas, M.A. Salam and S. S. Al-Juaid, Prog. Org. Coat., 2013, 76, 1810-1813.

[31] M. Abdel Salam, S.S. Al-Juaid, A.H. Qusti and A.A. Hermas, Synthetic Met., 2011, 161, 153-157.

[32] B. Zhang, Y. Xu, Y. Zheng, L. Dai, M. Zhang, J. Yang, Y. Chen, X. Chen and J. Zhou, Nanoscale Res. Lett., 2011 6,431-439.

[33] K.M. Kim, J.H. Kim, Y.Y. Lee and K.Y. Kim, Int. J. Hydrogen Energ., 2012, 37, 1653-1660.

[34] V.D. Patake and C.D. Lokhande, Appl. Surf. Sci., 2008, 254, 2820-2824.

[35] J. Wen and Z. Zhou, Mater. Chem. Phys., 2006, 98, 442-446.

[36] W.C Fang, J.H. Huang, L.C. Chen, Y.L. Oliver Su and K.H. Chen, J. Power Sources, 2006, 160, 1506-1510.

[37] Z. He, L. Liu, C. Gao, Z. Zhou, X. Liang, Y. Lei, Z. He and S. Liu, RSC Adv., 2013, 3, 19774-19777.

[38] P. Han, X. Wang, L. Zhang, T. Wang, J. Yao, C. Huang, L. Gu and G. Cui, RSC Adv., 2014, 4, 20379-20381.

[39] C. Flox, C. Fabrega, T. Andreu, A. Morata, M. Skoumal, J. Rubio-Garciaand J.R. Morante, RSC Adv., 2013, 3, 12056-12059.

[40] H. Zhou, J. Xi, Z. Li, Z.Zhang, L. Yu, L. Liu, X. Qiu and L. Chen, RSC Adv., 2014, DOI: 10.1039/c0xx00000x.

[41] H. Liu, L. Yang, Q. Xu and C. Yan, RSC Adv., 2014, DOI: 10.1039/C4RA09777G.

[42] Z. Gonzalez, C. Botas, P. Alvarez, S. Roldan, C. Blanco, R. Santamarıa, M. Granda and Rosa Menendez, Carbon, 2012, 5 0, 828-834.

[43] Q. Xu, T.S. Zhao, L. Wei, C. Zhang and X.L. Zhou, Electrochim. Acta, 2015, 154, 462-467.

[44] P. Han, H. Wang, Z. Liu, X. Chen, W. Ma, J. Yao, Y. Zhu and G. Cui, Carbon, 2011, 49, 693-700.

[45] C. Flox, M. Skoumal, J. Rubio-Garcia, T. Andreu and J.R. Morante, Appl. Energ., 2013, 109, 344-351.

[46] G. Wei, C. Jia, J. Liu, and C. Yan, J. Power Sources, 2012, 220, 185-192.

**Figure captions**

Fig.1. SEM images of MWCNT/SSM electrode (a), MWCNT/SSM electrode with high magnification (b), $RuO_2$/MWCNT/SSM electrode (C) and EDX spectra obtained of $RuO_2$/MWCNT/SSN electrode (d), XRD patterns of $RuO_2$/MWCNT/SSM electrode (e).

Fig.2. Cyclic voltammogram of the MWCNT/SSM electrode deposited with and without $RuO_2$ in 0.14 M $[VO_2]^+$ + 2 M $H_2SO_4$ at a scan rate of 20 mV $s^{-1}$(a), The presumed catalytic mechanism of $RuO_2$/MWCNT/SSM toward $VO_2^+/VO^{2+}$ (b)

Fig.3. Impedance Nyquist plots of the MWCNT/SSM and the $RuO_2$/MWCNT/SSM electrode in 0.14 M $[VO]^{2+}$ + 0.14 M $[VO_2]^+$ + 2 M $H_2SO_4$ solution at the open-circuit potential.

Fig.4. Cyclic voltammograms plots at various scan rates in 0.14 M $[VO_2]^+$ + 2 M $H_2SO_4$ for the $RuO_2$/MWCNT/SSM electrode (a), The plot of peak current $I_p$ as a function of square of scan rate for $VO^{2+}/VO_2^{+1}$ redox(b).

Fig.5. The cyclic voltammograms of $RuO_2$/MWCNT/SSM electrode in 2 M $H_2SO_4$ solution with different concentrations of $[VO]^{2+}/[VO_2]^+$ at a potential sweep rate of 20 mV $s^{-1}$ (a), The plot of peak current $I_p$ as a function of concentration of $[VO]^{2+}/[VO_2]^+$ (b).

Fig.6. Galvanostatic charge/discharge cycling curves of $RuO_2$/MWCNT/SSM and MWCNT/SSN electrode in 0.14 M $[VO]^{2+}$ + 0.14 M $[VO_2]^+$ + 2 M $H_2SO_4$ solution at the current density of 500 mA $g^{-1}$. $[VO]^{2+}/[VO_2]^+$

Fig.7. Galvanostatic charge/discharge cycling curves at different current densities in 0.14 M $[VO]^{2+}$ + 0.14 M $[VO_2]^+$+ 2 M $H_2SO_4$ for the $RuO_2$/MWCNT/SSM electrode.

Fig.8. Charge/discharge curves of the $RuO_2$/MWCNT/SSM electrode in 0.14 M $[VO]^{2+}$ + 0.14 M $[VO_2]^{+}$ + 2 M $H_2SO_4$ solution at the current density of 500 mA $g^{-1}$ for the first and 10th dyes.

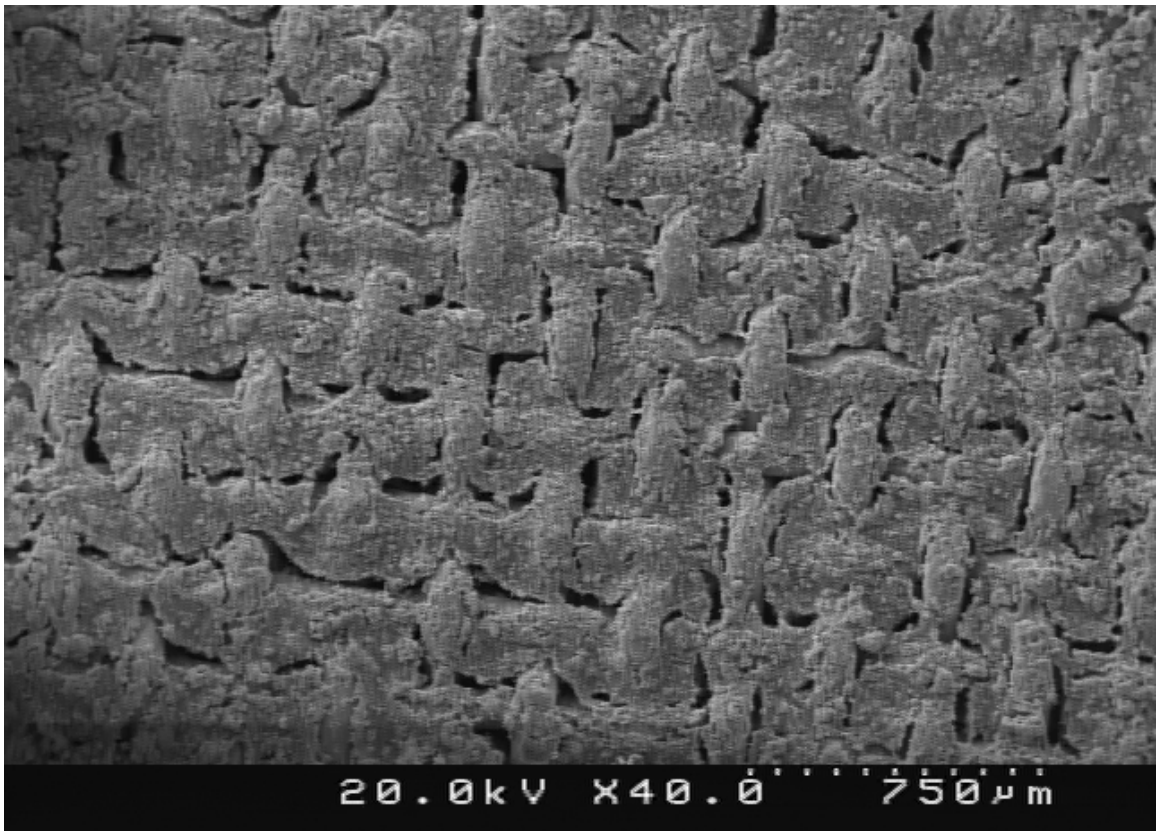


**Figure 1a**

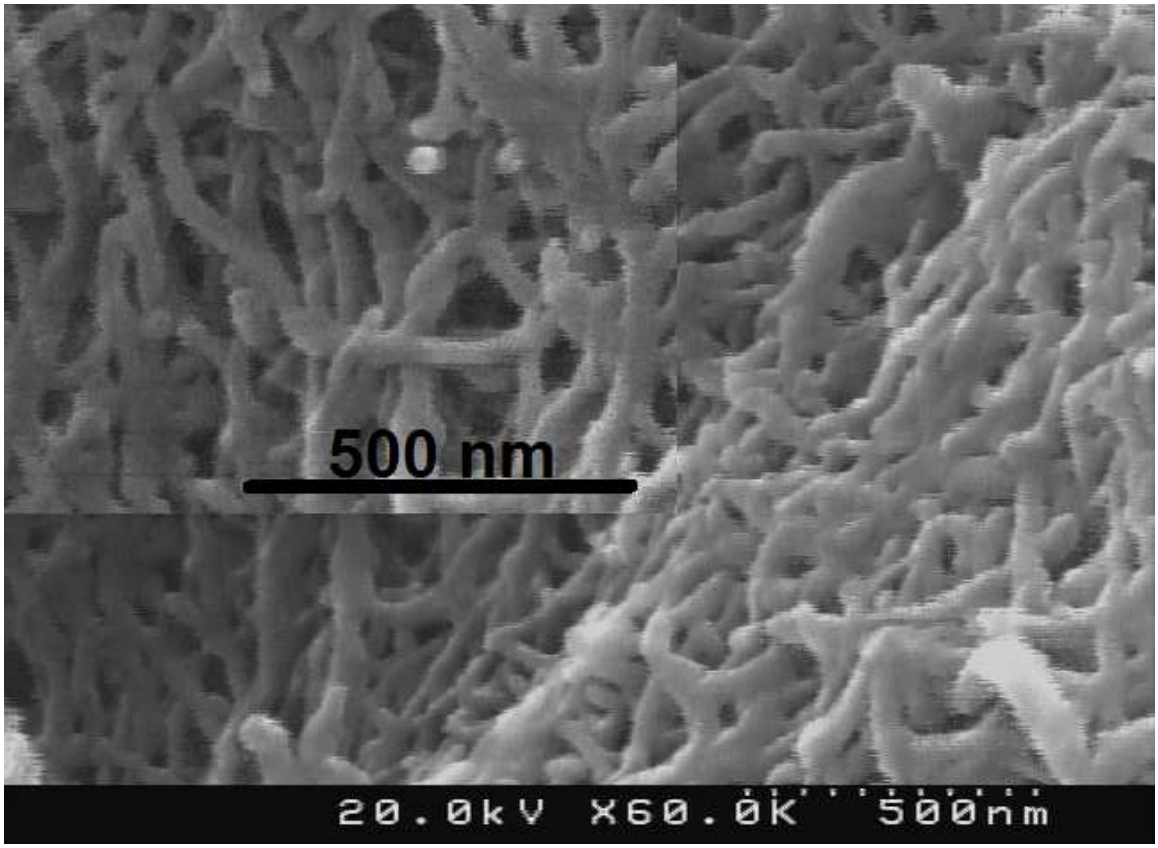


**Figure 1b**

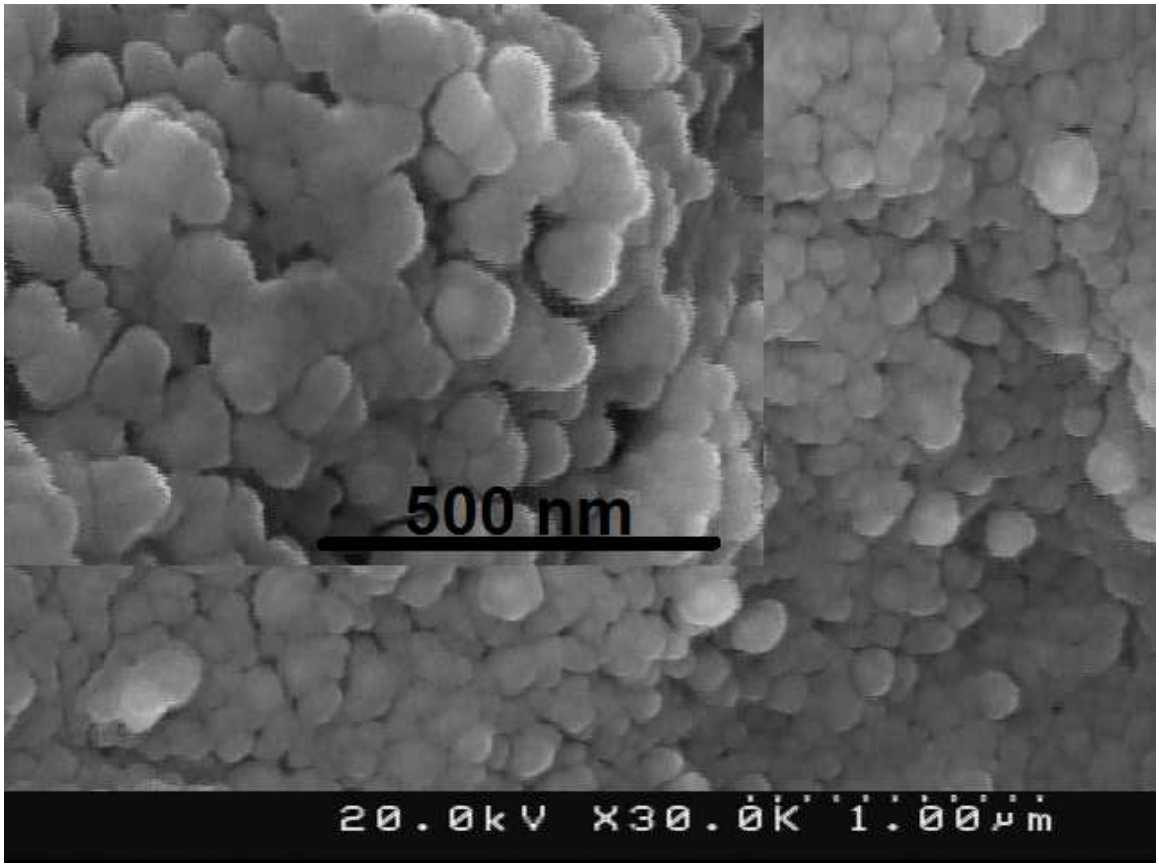


**Figure 1c**

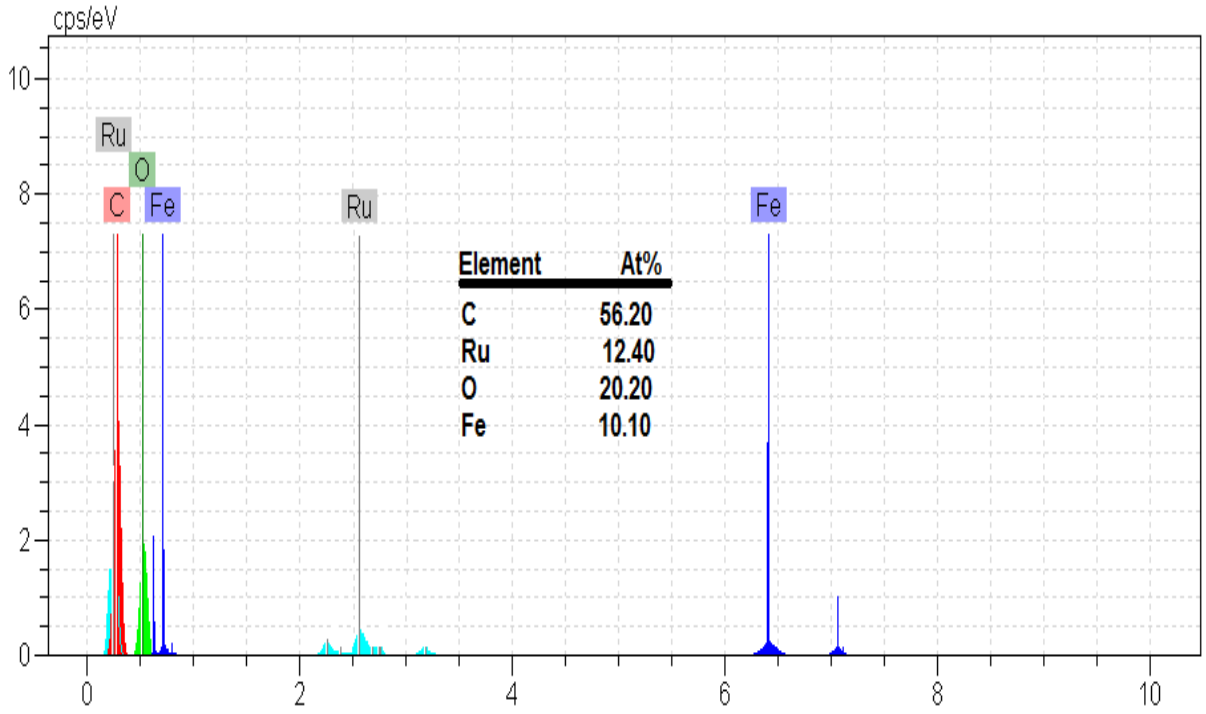


**Figure 1d**

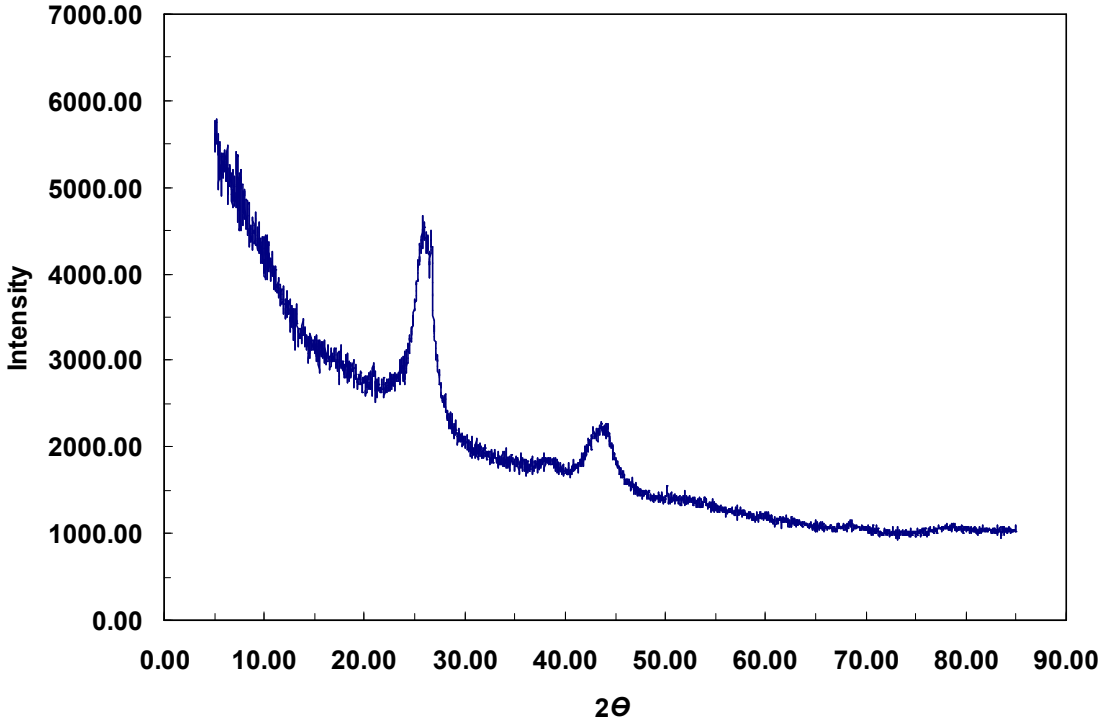


**Figure 1e**

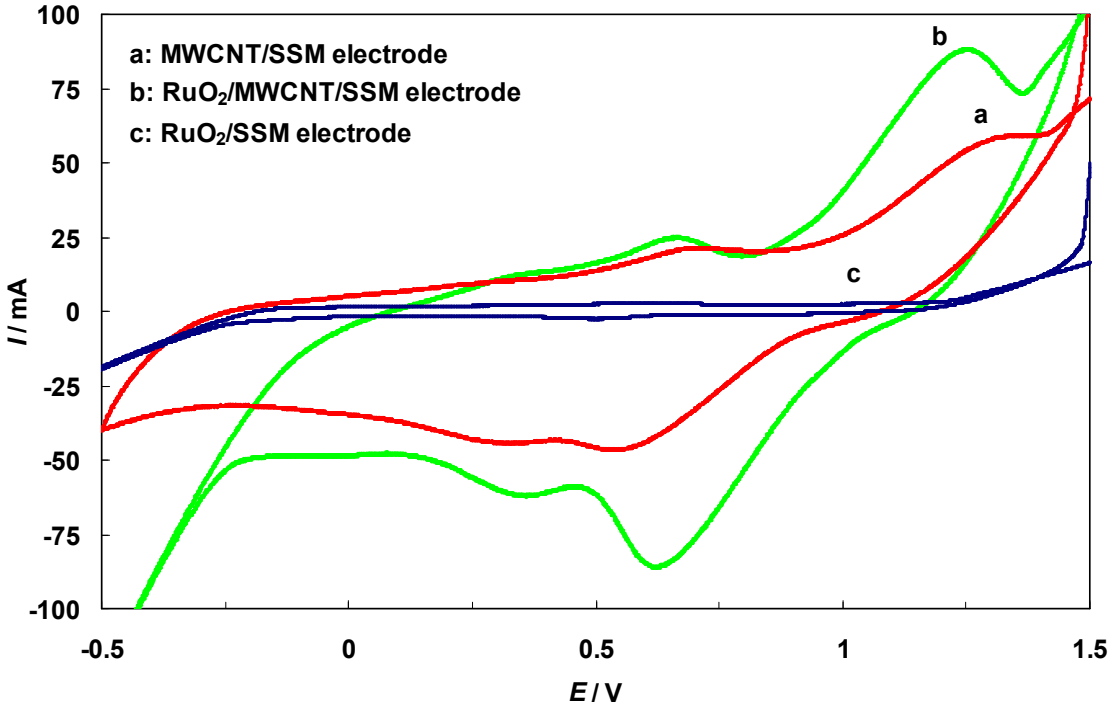


**Figure 2a**

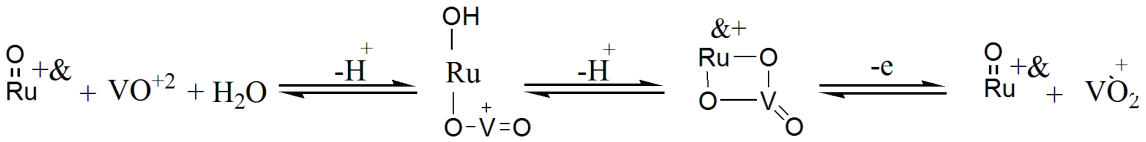

**Figure 2b**

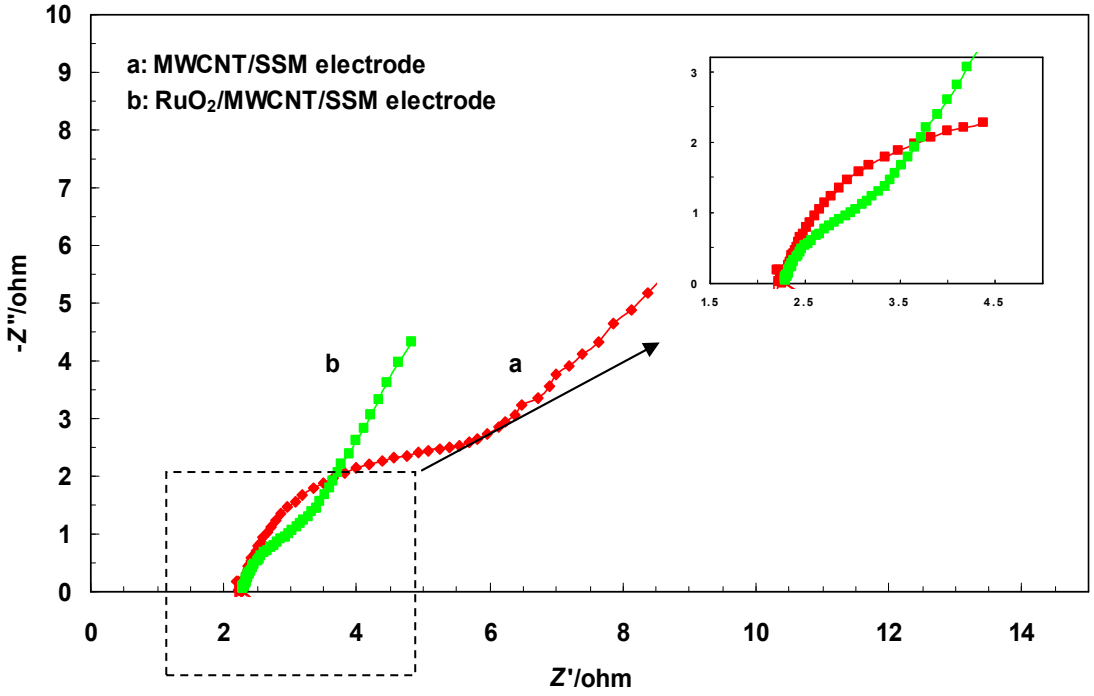


**Figure 3**

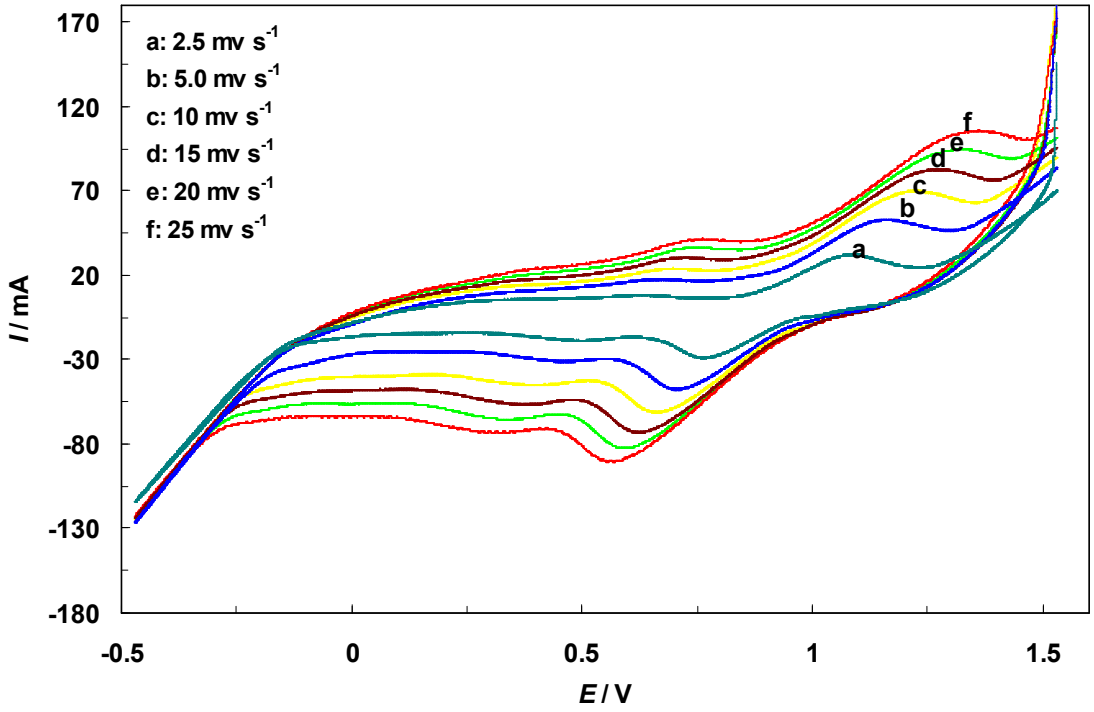


**Figure 4a**

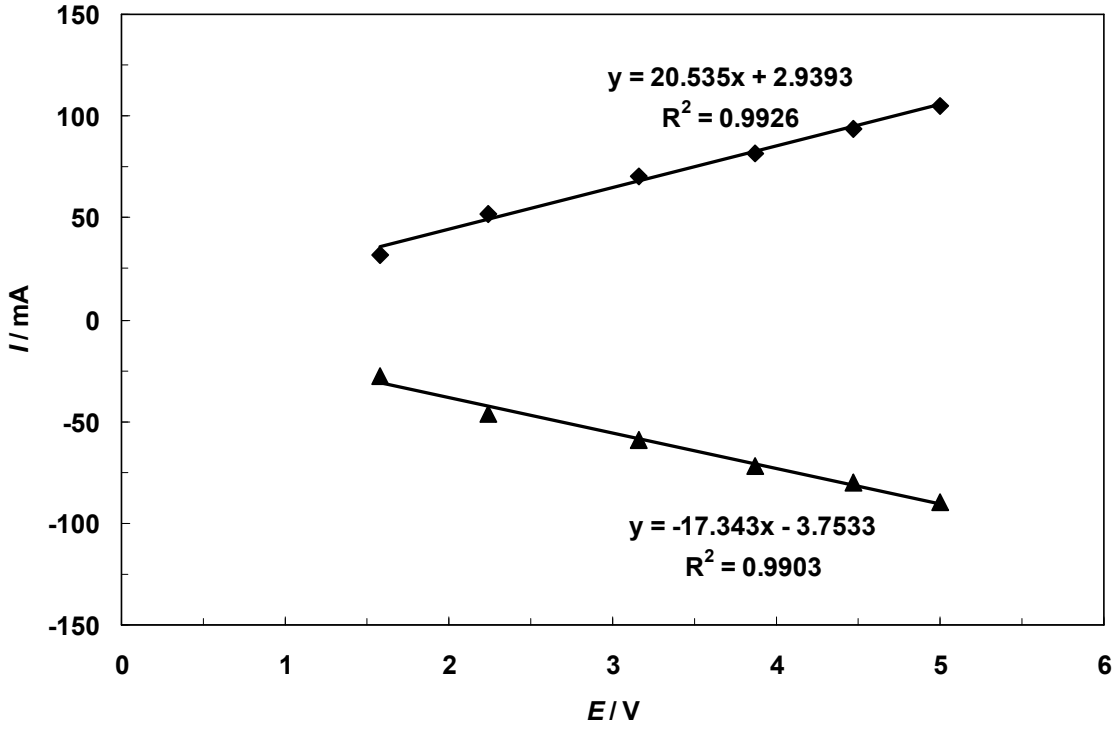


**Figure 4b**

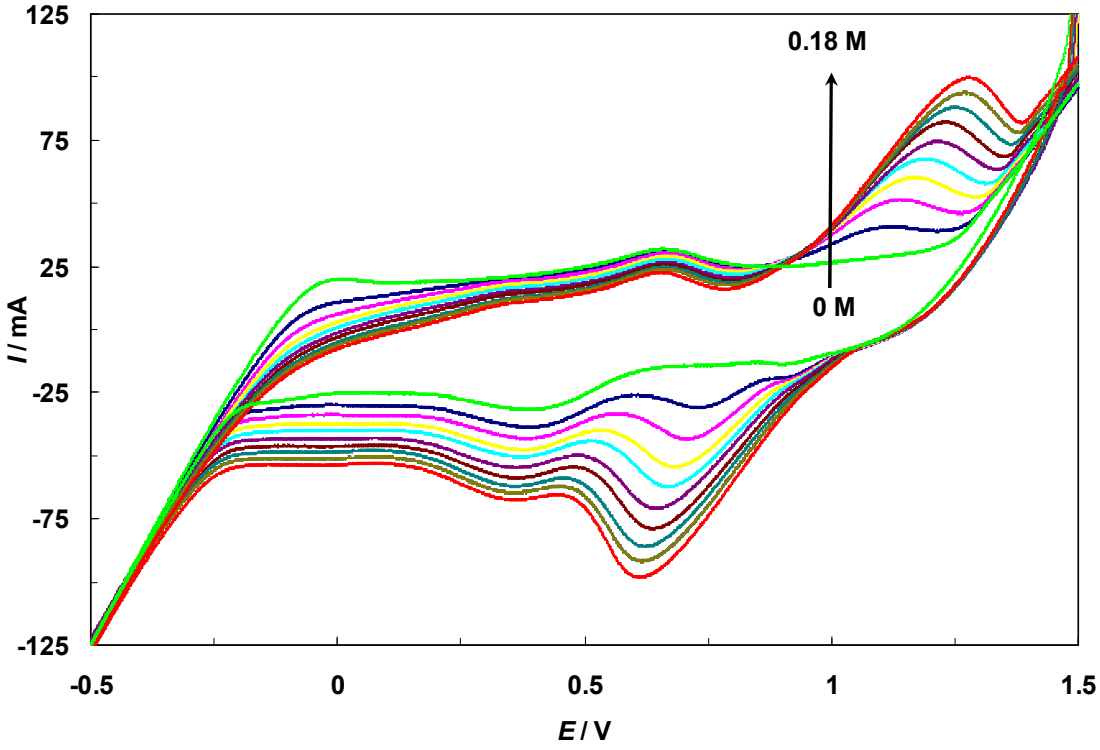


**Figure 5a**

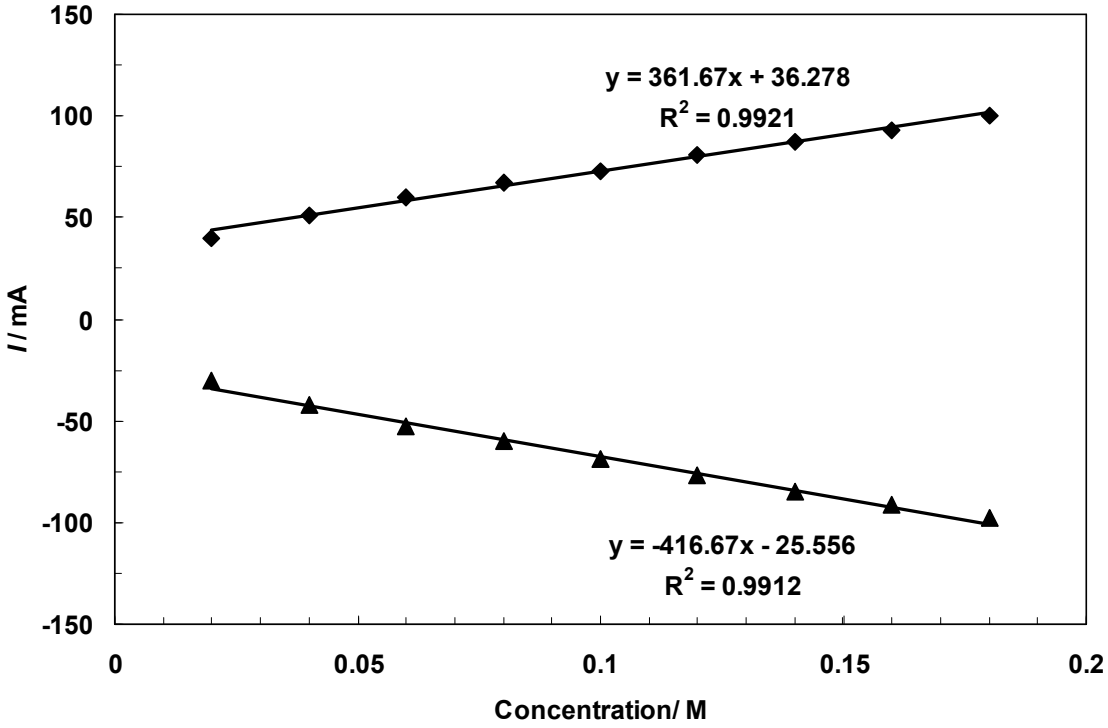


**Figure 5b**

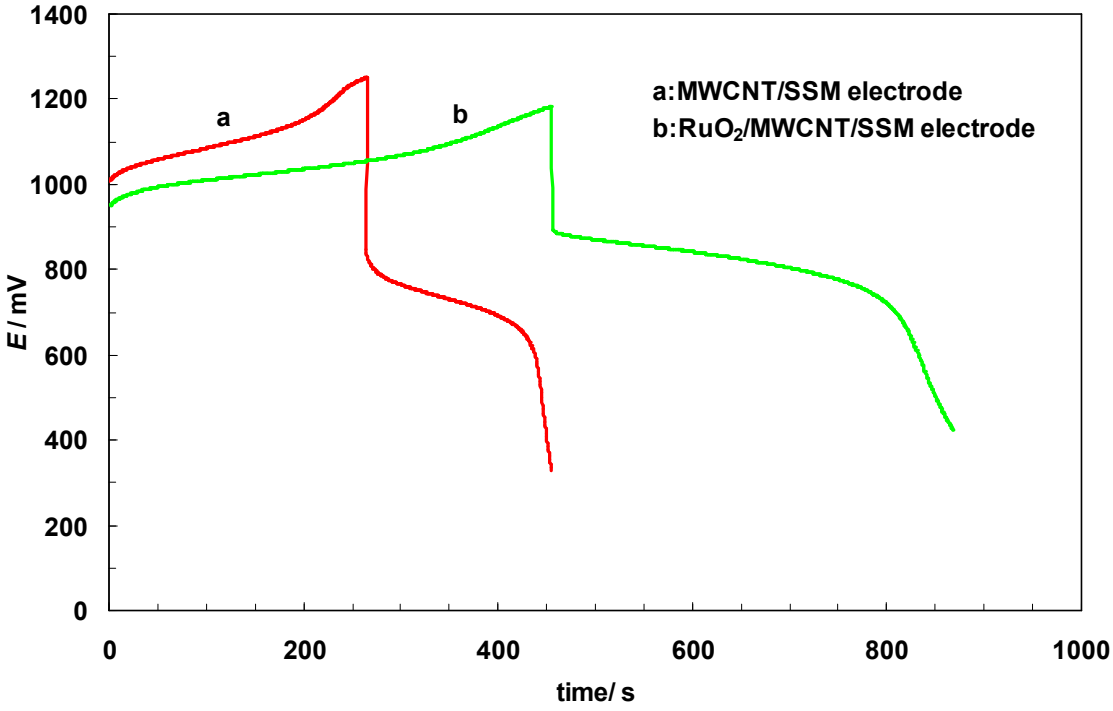


**Figure 6**

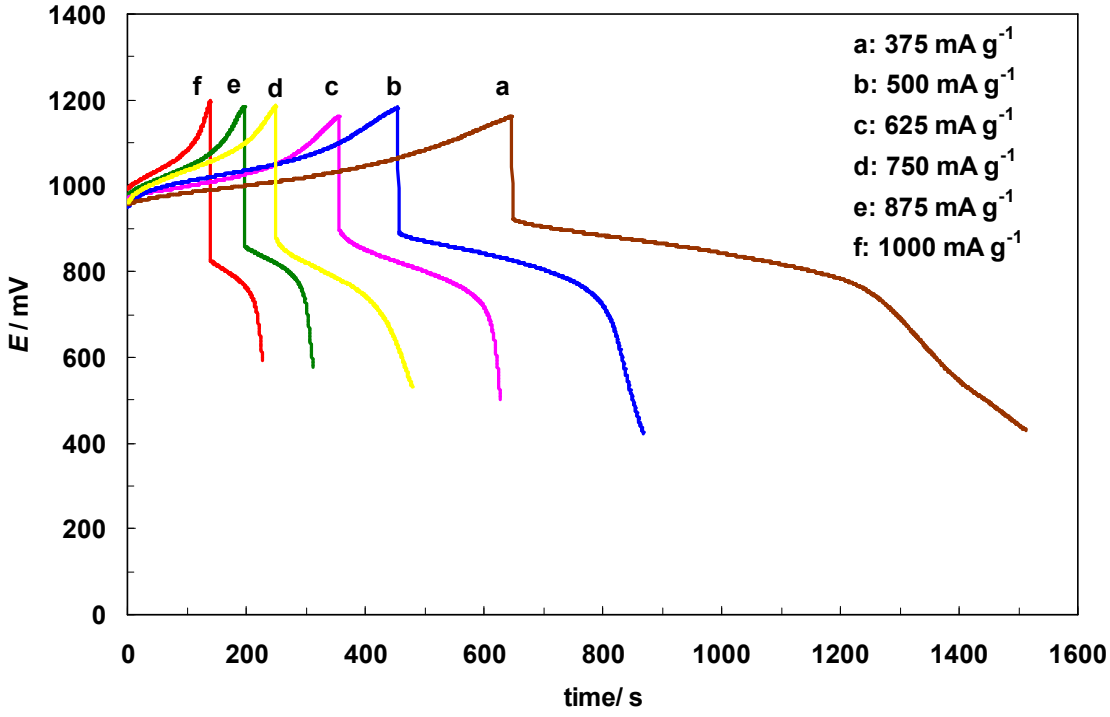


**Figure 7**

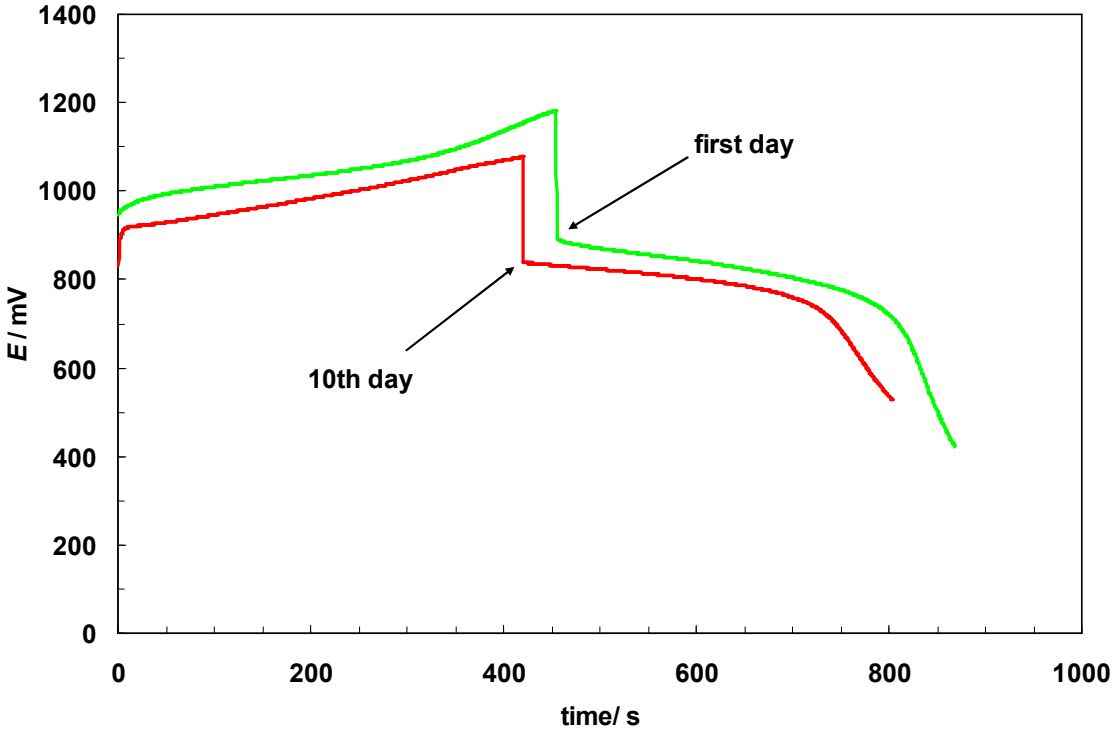


**Figure 8**